

Highly zone-dependent synthesis of different carbon nanostructures using plasma-enhanced arc discharge technique

Rajesh Kumar · Rajesh Kumar Singh · Pawan Kumar Dubey ·
Ram Manohar Yadav · Dinesh Pratap Singh ·
R. S. Tiwari · O. N. Srivastava

Received: 23 July 2014 / Accepted: 18 December 2014 / Published online: 13 January 2015
© Springer Science+Business Media Dordrecht 2015

Abstract Three kinds of carbon nanostructures, i.e., graphene nanoflakes (GNFs), multi walled carbon nanotubes (MWCNTs), and spherical carbon nanoparticles (SCNPs) were comparatively investigated in one run experiment. These carbon nanostructures are located at specific location inside the direct current plasma-assisted arc discharge chamber. These carbon nanomaterials have been successfully synthesized using graphite as arcing electrodes at 400 torr in helium (He) atmosphere. The SCNPs were found in the deposits formed on the cathode holder, in which highly curled graphitic structure are found in majority. The diameter varies from 20 to 60 nm and it also appears that these particles are self-assembled to each other. The MWCNTs with the diameter of 10–30 nm were obtained which were present inside the swelling portion of cathode deposited. These MWCNTs have 14–18 graphitic layers with 3.59 Å interlayer spacing.

The GNFs have average lateral sizes of 1–5 μm and few of them are stacked layers and shows crumpled like structure. The GNFs are more stable at low temperature (low mass loss) but SCNPs have low mass loss at high temperature.

Keywords Graphene nanoflakes · Zone dependent temperature · Arc discharge · Local defect

Introduction

Carbon nanomaterials have a number of current and potential future applications due to their highly stable physicochemical properties, low cost, good conductivity, and high porous surface area. These carbon nanomaterials present a wide range of applications

R. Kumar (✉)
Department of Materials Science & Engineering, Yonsei
University, Seoul 120-749, Republic of Korea
e-mail: rajeshbhu1@gmail.com

R. Kumar · R. S. Tiwari · O. N. Srivastava
Department of Physics, Banaras Hindu University,
Varanasi 221005, India

R. K. Singh (✉)
Department of Applied Physics, Indian Institute of
Technology, Banaras Hindu University, Varanasi 221005,
India
e-mail: rksbhu@gmail.com

P. K. Dubey
Nanotechnology Application Centre, University of
Allahabad, Allahabad 211002, India

R. M. Yadav
Department of Materials Science and Nano Engineering,
Rice University, Houston, TX 77005, USA

D. P. Singh
Departamento de Física, Universidad de Santiago de
Chile, Avenida Ecuador 3493, Estación Central,
9170124 Santiago, Chile

including fuel cells, field emission devices, hydrogen storage, supercapacitors, sensors, and battery electrodes (Endo et al. 2001; Milne et al. 2004; Yoshitake et al. 2002). Among many methods that have been applied to obtain carbon materials are arc discharge method (Subrahmanyam et al. 2009), laser ablation method, solvothermal method (Choucair et al. 2009), and chemical vapor deposition (Wang et al. 2009). Among these available methods, the arc discharge method is most widely used because of its simplicity and cost-effective technology compared to other more expensive ones (Gattia et al. 2007; Li et al. 2010). In arc discharge method, arc current, ambient gas, and ambient pressure inside the arcing chamber are the important parameters for synthesis of different carbon nanostructures (Kim et al. 2012). The direct current (DC) arc supplies sufficient energy in form of temperature to electrode causing the evaporation and formation of arc plasma. A high influx of plasma species and high temperature play key role in the growth of carbon nanostructures. Economically feasible large-scale production and purification techniques still have to be developed for the synthesis of carbon nanostructures. Different types of carbon related nanostructure such as nanotubes (Liang et al. 2012; Sun et al. 2013), carbon nanoparticles (Borgohain et al. 2014; Xing et al. 2007), graphene nanoflakes (GNFs) (Li et al. 2013; Wu et al. 2010) and other types of carbon nanostructure materials e.g., fullerenes (Churilov 2008) can be produced using arc discharge method.

It is widely recognized that plasma enhance arc discharge method will be one of the most promising means for the production of carbon-based nanostructures. Therefore, a simple and systematic study, dealing with the identification of key parameters that allow to control the carbon-based nanostructure, is required. Some studies (Bagiante et al. 2010; Scalese et al. 2010; Scuderi et al. 2009) have shown that the electrode shape and size, ambient pressure and the arcing current greatly influence the nature or type and quality of carbon-based nanostructure.

In this work, we have investigated the effect of temperature on the carbon product synthesized after arcing the graphite electrode in helium (He) atmosphere. Soot samples were collected from different axial and top locations inside the arc discharge chamber to study soot structure, size, graphitization, and agglomeration using transmission electron microscopy (TEM) and HRTEM. Furthermore, by

investigating the morphologies and microstructures of the cathode deposits and evaporated soot, we have found that different carbon nanostructures have been formed at different locations and similar nanostructures were formed at specific locations. A suitable mechanism has been provided for the different carbon nanomaterials formed.

Experimental section

Synthesis of carbon-based nanostructures

The direct current (DC) arc discharge of graphite electrode was carried in the same apparatus as reported previously (Kumar et al. 2013). The cylindrical cathode rod was ($L = 15$ mm, $\varnothing = 5$ mm) sharp end toward the anode in order to decrease the formation of cathode deposition. The anode rod was rectangular ($20 \times 8 \times 8$ mm³) for large amount of carbon shoot evaporation. The cathode was fixed in the apparatus, and the anode can be moved toward the cathode. This method creates soots through arc-vaporization of two graphitic rods placed end to end, separated by approximately 1 mm, in an enclosure that is usually filled with inert gas (helium, argon) at low pressure (between 50 and 700 mbar). The anode gets evaporated after ignition of the plasma due to the high heat flux from the DC arc discharge. The electric arc was generated (30 V, 100 A) in a helium atmosphere at 400 torr. During the arcing, the distance between two graphite electrodes was maintained constant by continuously translating the anode rod toward cathode. After the complete evaporation, the black carbon shoots like materials were collected from different regions of the experimental apparatus and were characterized.

Characterization

Black carbon shoots like materials were characterized using X-ray diffractometer (XRD) (Philips PW 1710), scanning electron microscopy (SEM) (Philips XL 20), transmission electron microscopy (HRTEM) (Tecnai 20 G²), and Raman spectroscopy. Sample for TEM studies were prepared by dispersing a small amount of material in ethanol with sonication for 5 min. Drops of the dispersion were placed onto a holey carbon grid and dried. Raman spectrum of as-grown sample was measured by Raman spectrometer (Renishaw, model

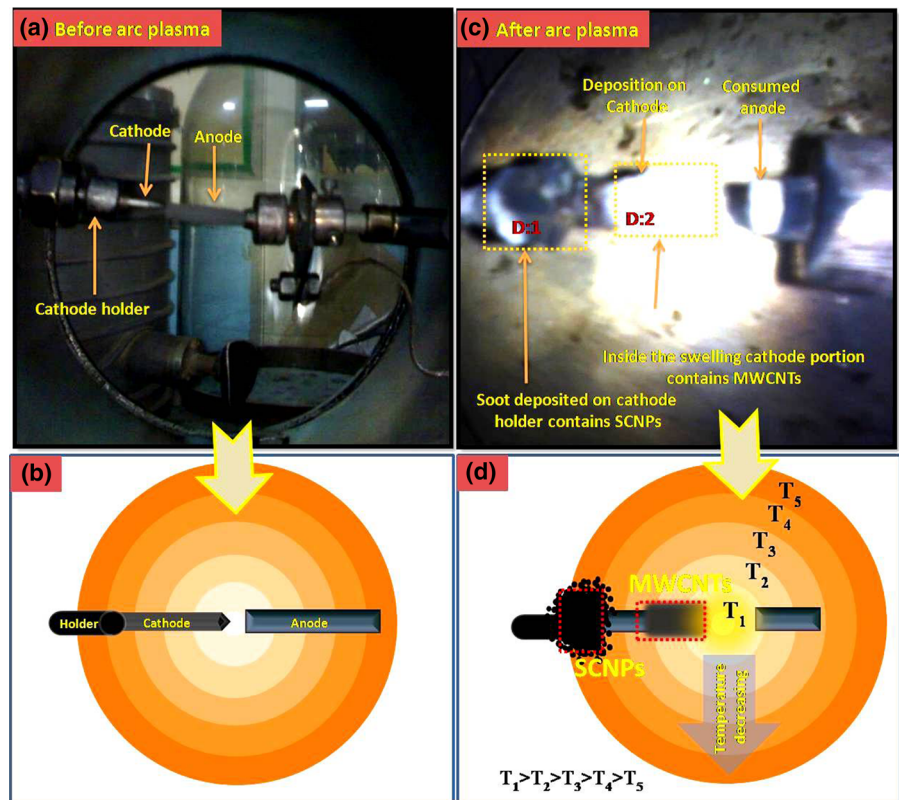
no. H 45517) using an argon ion laser ($\lambda = 514 \text{ nm}$). The thermal stability of different carbon nanostructures formed was measured by the thermal gravimetry analysis (TGA) (STA 449F3) from 32 to 850 °C at the rate of 10 °C/min under oxygen ambience.

Result and discussion

In the arc evaporation of graphite, only anode was consumed by the dc arc discharge. The consumption rate of anode was measured to be 3.5 mgs^{-1} . After the complete DC arc discharge, sample was collected from three different parts of the arc chamber. Deposit-1 (D:1) is the sample deposited on the cathode holder, deposit-2 (D:2) is its cathode swelling containing portion (consumed part of anode), and deposit-3 (D:3) (not shown in Fig. 1b) was the fine powder sticks on the upper portion of the arc chamber. The shape of the solid product is schematically described in Fig. 1. A series of analytical experiments were carried out in order to determine the composition and structure of the generated different carbon nanostructures.

In order to investigate the effect of deposits sites on the product in the arc discharge method, the products obtained from different regions were investigated. After the SEM characterization, these images include three typical soot's like structures which were deposited on the cathode holder (D:1), deposited on the tip of cathode (D:2) and deposited on the upper portion of chamber (D:3, along the vertical direction). Figure 2a–c shows SEM images of carbon materials which contains different morphological nanostructures. The investigated morphology contains agglomerated spherical carbon nanoparticles (SCNPs) (D:1), MWCNTs (D:2), and GNFs (D:3). It was observed that the carbon soot deposited on the cathode holder contains only aggregates of small SCNPs and some nanoparticles are connected with each other as shown in Fig. 2a. The samples from D:2 and D:3 contains multi walled carbon nanotubes (MWCNTs) (Fig. 2b) and GNFs (Fig. 2c), respectively. Arc discharge between anode and cathode was done for 2 min and 30 s. The yield of the SCNPs, MWCNTs, and GNFs are 210, 155, and 95 mg, respectively.

Fig. 1 Optical and schematic temperature profile of arc discharge



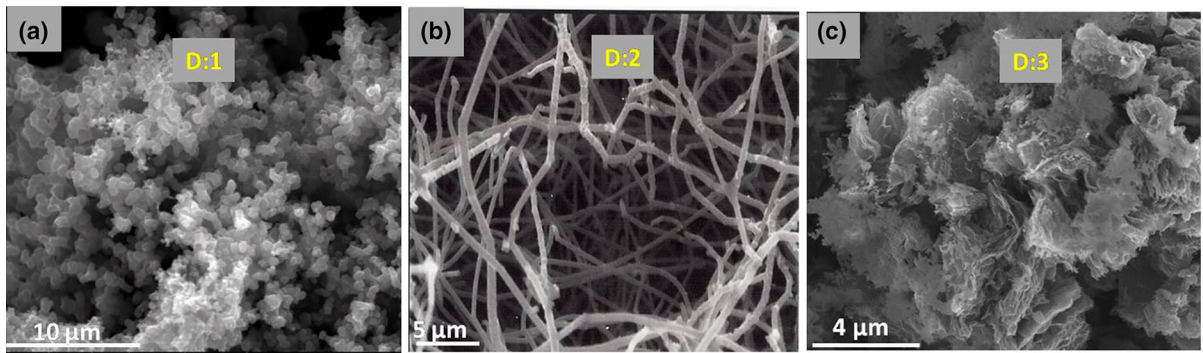


Fig. 2 SEM micrographs of **a** SCNPs, **b** MWCNTs, and **c** GNFs

TEM characterization also indicates that the main products observed were SCNPs, MWCNTs, and GNFs. The typical transmission electron microscope image of the SCNPs can be seen in Fig. 3a, b. The diameter of SCNPs was found in nano dimension (Fig. 3a, b) and it shows that some particles are

agglomerated and some are connected to each other. From the micrographs, it is also possible to estimate the SCNPs size which varies from 20 to 60 nm and all SCNPs are having the similar structures. The histogram in the inset of Fig. 3b shows the diameter distribution of SCNPs. These SCNPs aggregate

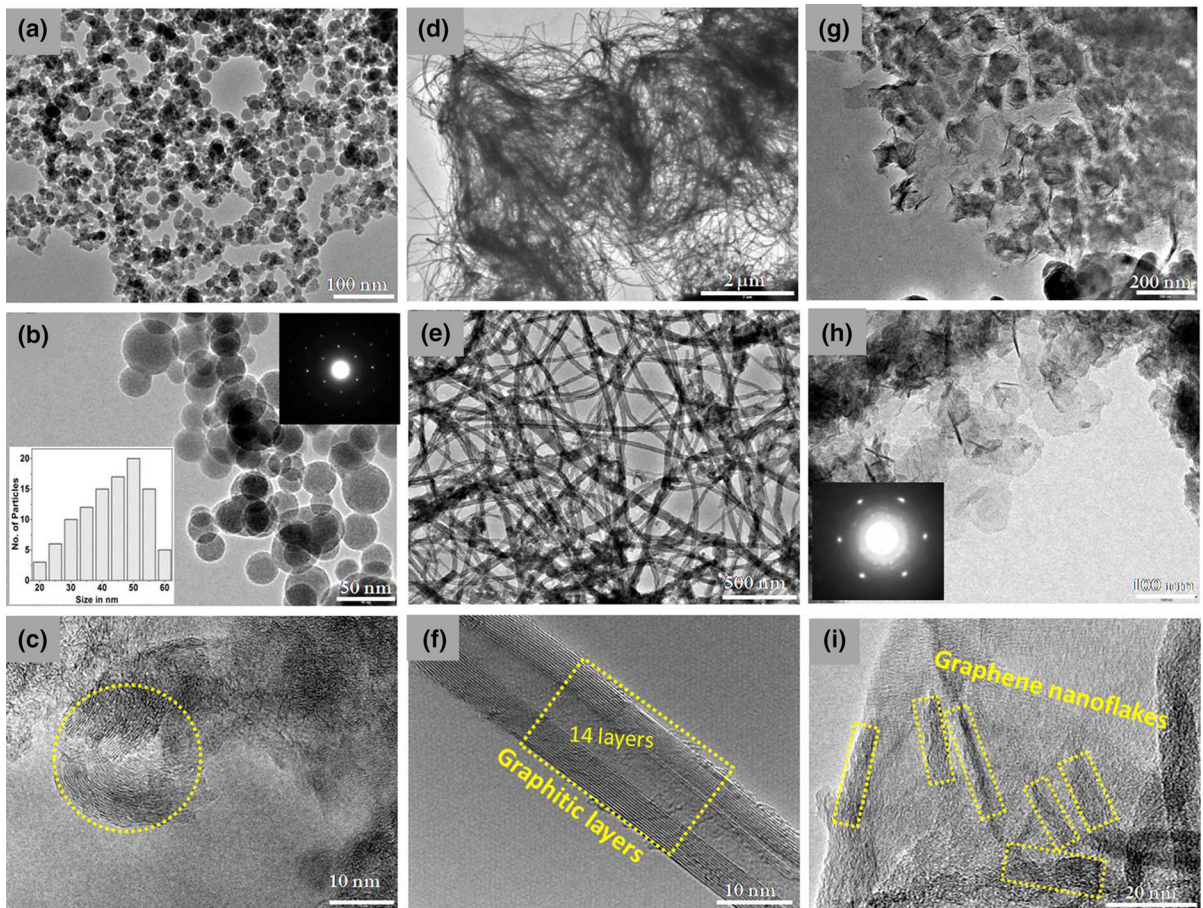


Fig. 3 TEM micrographs at different magnifications as **a–c** SCNPs, **d–f** MWCNTs, and **g–i** GNFs

linearly and form chained structures and also appears as necklace type chain which contains SCNPs. The growth process takes place at a relatively low plasma temperature as comparison to MWCNTs and GNFs. This induces the nearly isotropic growth of SCNPs. These spheres are crystalline, as shown in HRTEM images (Fig. 3c). The crystalline nature has been also confirmed by the electron diffraction pattern in the inset of Fig. 3b. Figure 3d, shows the D:2 type of carbon soot which mainly contain MWCNTs nanostructure. These MWCNTs are entangled and having non-aligned structure as seen in TEM micrographs. The MWCNTs have nearly uniform diameter in the range of 5–20 nm. The representative high-resolution TEM (HRTEM) image of MWCNT shows 14 graphitic layer and more crystalline and nearly defects free structure as compared to SCNPs. Figure 3g–i show the typical TEM images of GNFs. Figure 3g, indicates that the third kind of deposition which was found on the dome was GNFs. The surface of the GNFs is not perfectly flat and shows different levels of transparency, which is similar to those synthesized by arc discharge in various environments (Chen et al. 2012; Hagino et al. 2012; Scuderi et al. 2012). Inset of Fig. 3h, shows the selected-area electron diffraction (SAED) pattern which indicates that GNFs is polycrystalline. In our experiment, it is indicated that these GNFs in the as-obtained sample consist of multi-layer graphene sheets. In addition, the average interlayer separations of the graphene sheets were 3.35 Å as determined by measuring the spacing of the dark fringes.

Figure 4 shows powder X-ray diffraction (XRD) patterns of as-synthesized carbon nanomaterials which were collected from different positions of arcing chamber. For instance, the (002) peak of samples prepared at is relatively broader and centered at $2\theta = 26.02^\circ$, 24.75° , and 26.56° , which corresponds to a graphitic interlayer spacing (d_{002}) of 3.42, 3.59, 3.35 Å for SCNPs, MWCNTs and GNFs, respectively. The other (100) peak at $2\theta = 44.7^\circ$ is present in SCNPs and MWCNTs but is not present in GNFs. The GNFs illustrated a weak peak corresponding to (002) lattice fringes at the diffraction angle of approximately 26.56° . It indicated a low graphitization degree and few layer graphene. The peaks of 002 reflections in SCNPs and MWCNTs are sharp as compared to GNFs, which implies that graphite sheets were regularly laminated and had an order structure in basal planes.

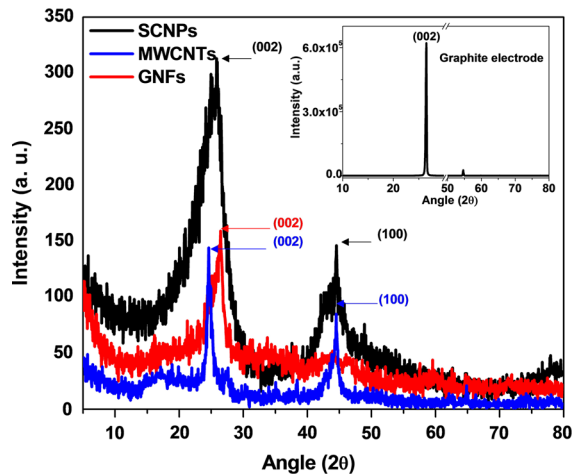


Fig. 4 XRD pattern of as synthesize SCNPs, MWCNTs, and GNFs

For comparison, the X-ray diffractogram of as used graphite electrode is characterized by a very sharp (002) diffraction peak 2θ and d-spacing value of $d_{002} = 3.35$ Å as shown in the inset of Fig. 4. All peaks are wider than that of a graphite electrode (inset Fig. 4) used for arcing to transform into carbon nanostructure.

Raman spectroscopy was performed to investigate the structures of SCNPs, MWCNTs, and GNFs by the resulting characteristic G and D bands which are sensitive to defects and disorder, respectively. Figure 5 shows the Raman spectra of as-synthesized carbon nanostructures. The Raman spectrum of

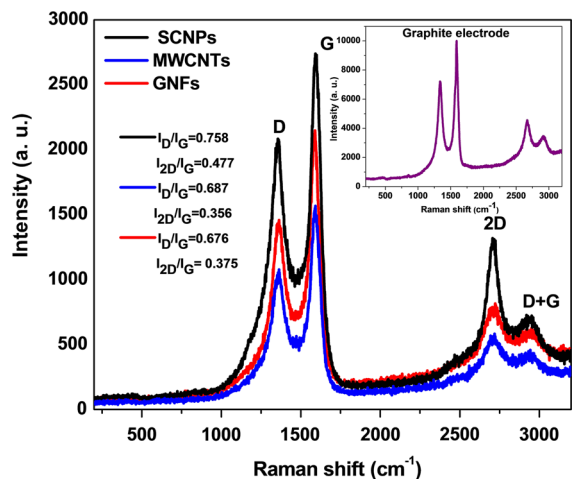


Fig. 5 Raman spectra of as-synthesized SCNPs, MWCNTs, and GNFs

carbon-based material is usually characterized by two main features: the G band (usually observed at $1,575\text{ cm}^{-1}$) and D band ($1,350\text{ cm}^{-1}$). The G band arises from the first order scattering of the E_{1g} phonon of sp^2 C atoms, while the D mode is a breathing mode of κ -point photons of A_{1g} symmetry (Chipara et al. 2013; Voronov and Street 2010). Thus, the G band is the result of vibration of sp^2 C atoms and the D band arises from the disorder and defect intensity of the crystal structure (Dresselhaus et al. 2004). An additional Raman line, found at about $2,709\text{ cm}^{-1}$ has been tentatively assigned as a G' band (or the D^* band or 2D band) (Dresselhaus et al. 2004). This is an overtone (2 phonon process) of the D band located between $2,450$ and $2,950\text{ cm}^{-1}$, and characterized by a width of about 81 , 100 and 109 cm^{-1} , corresponds to SCNPs, GNFs, and MWCNTs. The intensity ratio of D and G band (I_D/I_G) can be used to quantify the relative content of defects and the sp^2 domain size. Figure 5 shows the Raman spectra of SCNPs, MWCNTs, and GNFs carbon-based nanostructures. A broad D and G band are present in all of them. The I_D/I_G for SCNPs, MWCNTs, and GNFs is ~ 0.758 , 0.687 and 0.676 , respectively. The relative intensities in Raman spectra of the D band to the G band (I_D/I_G) and the 2D band to the G band (I_{2D}/I_G) for SCNPs, MWCNTs, and GNFs have been shown in Fig. 6. According to the trend in I_D/I_G ratio, it is confirmed that GNFs have the minimum disorder structure and SCNPs have the maximum disorder structure in the collected soot materials inside the arc chamber. The degree of graphitization increases from SCNPs to MWCNTs to GNFs. The result demonstrates that more defects have

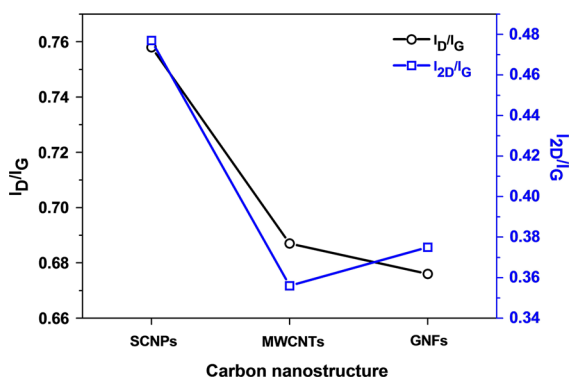


Fig. 6 The relative intensities in Raman spectra of the D band to the G band (I_D/I_G) and the 2D band to the G band (I_{2D}/I_G) for SCNPs, MWCNTs, and GNFs

been introduced into the SCNPs carbon-based nanostructures.

For surface composition and elemental analysis, the SCNPs, MWCNTs, and GNFs were further characterized by X-ray photo electron spectroscopy (XPS). Figure 7 shows the XPS spectra of as-synthesized carbon nanostructure. Figure 7a shows the evolution of the C1s spectra while Fig. 7b contains the corresponding O1s spectra of as-synthesized carbon-based nanostructures. In the Fig. 7a, C1s spectra consists of one components, at binding energy 284.7 eV which features the $C=C\ sp^2$ bonds in the graphitic network, one at 285.3 eV which is attributed to carbon bonds with sp^3 hybridization. The O1s spectrum (Fig. 7) showed one peaks at 535.4 eV , which was attributed to $COO-$ bands.

Thermal gravimetri analysis (TGA) data can give indication for the presence of carbonaceous impurities such as amorphous carbon and graphite, the thermal stability of carbon and purity of the carbon nanostructure. For every case, TGA analysis was done up to $850\text{ }^\circ\text{C}$ to evaluate the thermal stability and purity of the carbon black soot powder collected from different places. TGA curve of SCNPs, MWCNTs, and GNFs are shown in Fig. 8, which suggests a single weight-loss related to the burning of raw carbon nanostructures. In this experimental work, the TGA analysis was performed in oxygen ambient, with a temperature increase of $10\text{ }^\circ\text{C}/\text{min}$. Figure 8 shows the profiles for the as-synthesized SCNPs, GNFs, and MWCNTs. Nearly, 87.3% weight loss was seen in MWCNTs and GNFs at $800\text{ }^\circ\text{C}$. But, in case of SCNPs, it was 71.3% of the initial weight. TGA analysis indicates that there is no significant weight loss below 180 , 350 and $500\text{ }^\circ\text{C}$ for SCNPs, MWCNTs and GNFs, respectively. However, SCNPs, MWCNTs, and GNFs start to lose mass above 180 , 350 and $500\text{ }^\circ\text{C}$ and we found a sharp decline in weight loss in the range of $500\text{--}800\text{ }^\circ\text{C}$ (single-step decomposition of carbon black powder); this can be attributed to the oxidation behavior of carbonaceous material. The SCNPs and MWCNTs do not shows the sharp decline in weight loss as compared to GNFs. The above analysis shows that the oxidation temperature and thermal stability of GNFs are higher as compared to SCNPs and MWCNTs.

Figure 9 shows the schematic presentation of three kinds of carbon nanostructures. In arc discharge processes, very high temperature gets generated

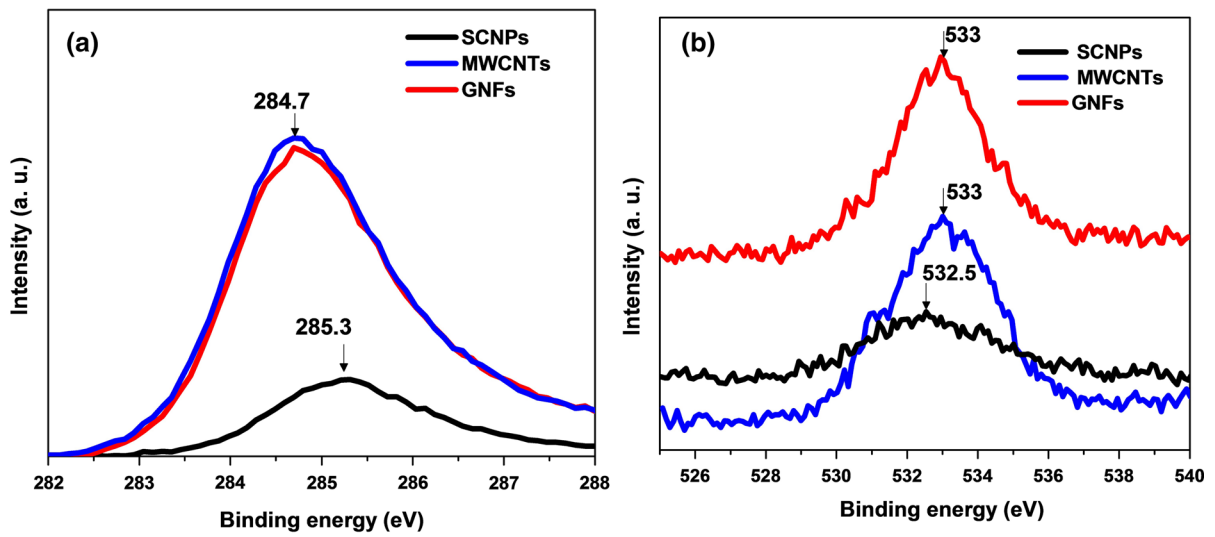


Fig. 7 a C1s and b O1s XPS core level spectra of as-synthesized SCNPs, MWCNTs, and GNFs

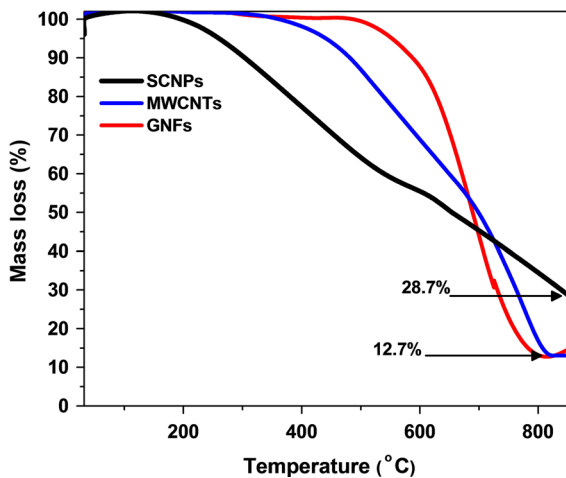


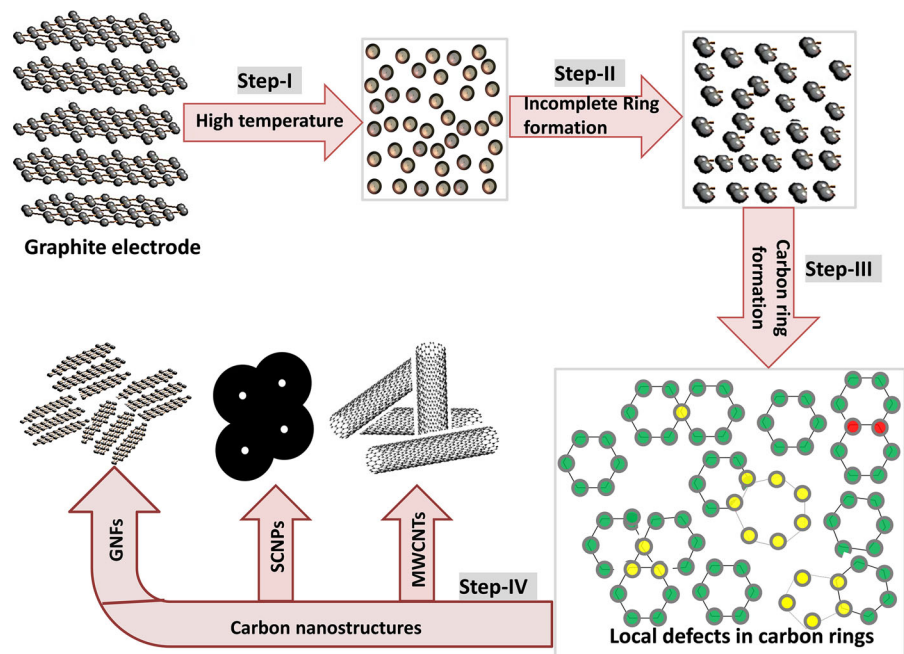
Fig. 8 TGA analysis of as-synthesized SCNPs, MWCNTs, and GNFs

between the closely separated graphite electrodes. Due to the high temperature, carbon atoms start to dissociate from graphite electrodes (Huang et al. 2013). During arcing period, a given amount of the graphite is evaporated with different thermo-chemical reactions at high temperature and the vapor products are excited as carbon atoms or ions as shown in step-I. Step-II indicates that the evaporated atoms or ions starts to connect with each other in form of small carbon containing chain or carbon clusters and it depends upon the time stayed. These small carbons containing

chains or cluster gets fully transformed into hexagonal ring with some local defects as pentagonal, heptagonal, and other type of defect containing inside the new hexagonal graphitic structure as shown in step-III. These local defects inside hexagonal rings and temperature are responsible for folding and converting it into various carbon-based nanostructure as represent in step-IV. As we know that carbon heptagon/pentagon ring in graphitic materials is a key unit responsible for structural defects in sp^2 -hybridized carbon allotropes including SCNPs, MWCNTs, and GNFs.

Generally speaking, due to the plasma and heat outflow in the radial direction, the plasma density and temperature should have their highest value along the arc discharge centerline and decrease evidently along the radial direction (Beilis et al. 1999). We find that the temperature (at the least local temperature) for the MWCNTs formation is higher than that for SCNPs and GNFs. The local temperature on the tip edge of the deposited cathode, corresponding to the surrounding is higher. This implies that there are three completely different types of arc soot formed inside the arcing chamber. After arc evaporation, the nucleation and growth of small carbon clusters depend on the time stayed in the center of the arc field. We presume that the deposition place temperature is mainly responsible for the difference in microstructures. The temperature at cathode tip provide enough energy for rolling of

Fig. 9 Schematic formation of different carbon nanostructures



GNFs formed in arc plasma to form MWCNTs but when they reach on the upper chamber surface it gets cooled and are unable to roll and remained in the form of nanoflakes, which shows the GNFs structure. The smaller flacks deposited on the cathode holder (back-side to cathode) have also enough temperature to form the spherical microstructure such as SCNPs and attached to each other but that temperature is not enough to form the MWCNTs.

In lights of these results, we will further try to improve the working chamber system by designing the concentric spherical mesh around the arcing site so that isothermal condition is satisfied. Mesh will allow the evaporated material to go from it and allow to deposit on different isothermal platforms. Different carbon nanostructures will be further analyzed and their structures and morphologies will be studied.

Conclusions

We have successfully synthesized three types of carbon nanostructured were identified, and these nanostructures were highly assumed to depend on the specific locations inside the arcing chamber. The as produced carbon nanostructures are separately formed at different locations with different

nanostructures in single experiment, which is economically viable. SCNPs and MWCNTs are formed at cathode while GNFs are formed at the upper side of chamber wall of the arc discharge apparatus. The formation of these nanostructures are highly site dependent and we assumed that depositing place temperature play a key role in the change in nanostructures. These nanostructures are highly stable and the most stable nanostructure was found as GNFs as compared to SCNPs and MWCNTs.

Acknowledgments We would like to gratefully acknowledge anonymous referees for useful comments and constructive suggestions. Two of the authors, RKS and PKD are grateful to UGC-New Delhi for providing Dr D. S. Kothari Postdoctoral fellowship.

References

- Bagiante S, Scalese S, Scuderi V, D'Urso L, Messina E, Compagnini G, Privitera V (2010) Role of the growth parameters on the structural order of MWCNTs produced by arc discharge in liquid nitrogen. *Phys Status Solidi B* 247(4):884–887
- Beilis II, Keidar M, Boxman RL, Goldsmith S, Heberlein J, Pfender E (1999) Radial plasma flow in a hot anode vacuum arc. *J Appl Phys* 86(1):114–119

- Borghain R, Yang J, Selegue JP, Kim DY (2014) Controlled synthesis, efficient purification, and electrochemical characterization of arc-discharge carbon nano-onions. *Carbon* 66:272–284
- Chen Y, Zhao H, Sheng L, Yu L, An K, Xu J, Zhao X (2012) Mass-production of highly-crystalline few-layer graphene sheets by arc discharge in various H₂ inert gas mixtures. *Chem Phys Lett* 538:72–76
- Chipara DM, Macossay J, Ybarra AVR, Chipara AC, Eubanks TM, Chipara M (2013) Raman spectroscopy of polystyrene nanofibers-multiwalled carbon nanotubes composites. *Appl Surf Sci* 275:23–27
- Choucair M, Thordarson P, Stride JA (2009) Gram-scale production of graphene based on solvothermal synthesis and sonication. *Nat Nanotechnol* 4(1):30–33
- Churilov GN (2008) Synthesis of fullerenes and other nanomaterials in arc discharge. *Fuller Nanotub Carbon Nanostruct* 16:395–403
- Dresselhaus MS, Dresselhaus G, Jorio A (2004) Unusual properties and structure of carbon nanotubes. *Annu Rev Mater Res* 34:247–278
- Endo M, Kim YA, Hayashi T, Nishimura K, Matusita T, Miyashita K, Dresselhaus MS (2001) Vapor-grown carbon fibers (VGCFs): basic properties and their battery applications. *Carbon* 39(9):1287–1297
- Gattia DM, Antisari MV, Marazzi R (2007) AC arc discharge synthesis of single-walled nanohorns and highly convoluted graphene sheets. *Nanotechnology* 18(25):255604
- Hagino T, Kondo H, Ishikawa K, Kano H, Sekine M, Hori M (2012) Ultrahigh-speed synthesis of nanographene using alcohol in-liquid plasma. *Appl Phys Exp* 5(3):035101
- Huang L, Wu B, Chen J, Xue Y, Geng D, Guo Y, Yu G, Liu Y (2013) Gram-scale synthesis of graphene sheets by a catalytic arc-discharge method. *Small* 9(8):1330–1335
- Kim YA, Muramatsu H, Hayashi T, Endo M (2012) Catalytic metal-free formation of multi-walled carbon nanotubes in atmospheric arc discharge. *Carbon* 50(12):4588–4595
- Kumar R, Singh R, Ghosh AK, Sen R, Srivastava SK, Tiwari RS, Srivastava ON (2013) Synthesis of coal-derived single-walled carbon nanotube from coal by varying the ratio of Zr/Ni as bimetallic catalyst. *J Nano Res* 15(1):1–11
- Li N, Wang Z, Zhao K, Shi Z, Gu Z, Xu S (2010) Synthesis of single-wall carbon nanohorns by arc-discharge in air and their formation mechanism. *Carbon* 48(5):1580–1585
- Li Y, Chen Q, Xu K, Kaneko T, Hatakeyama R (2013) Synthesis of graphene nanosheets from petroleum asphalt by pulsed arc discharge in water. *Chem Eng J* 215–216:45–49
- Liang F, Shimizu T, Tanaka M, Choi S, Watanabe T (2012) Selective preparation of polyhedral graphite particles and multi-wall carbon nanotubes by a transferred arc under atmospheric pressure. *Diam Relat Mater* 30:70–76
- Milne WI, Teo KBK, Amaratunga GAJ, Legagneux P, Gangloff L, Schnell JP, Groening O (2004) Carbon nanotubes as field emission sources. *J Mater Chem* 14(6):933–943
- Scalese S, Scuderi V, Bagiante S, Simone F, Russo P, D'Urso L, Privitera V (2010) Controlled synthesis of carbon nanotubes and linear C chains by arc discharge in liquid nitrogen. *J Appl Phys* 107:014304
- Scuderi V, Scalese S, Bagiante S, Compagnini G, D'Urso L, Privitera V (2009) Direct observation of the formation of linear C chain/carbon nanotube hybrid systems. *Carbon* 47(8):2134–2137
- Scuderi V, Bongiorno C, Faraci G, Scalese S (2012) Effect of the liquid environment on the formation of carbon nanotubes and graphene layers by arcing processes. *Carbon* 50(6):2365–2369
- Subrahmanyam KS, Panchakarla LS, Govindaraj A, Rao CNR (2009) Simple method of preparing graphene flakes by an arc-discharge method. *J Phys Chem C* 113(11):4257–4259
- Sun L, Wang C, Zhou Y, Zhang X, Cai B, Qiu J (2013) Flowing nitrogen assisted-arc discharge synthesis of nitrogen-doped single-walled carbon nanohorns. *Appl Surf Sci* 277:88–93
- Voronov OA, Street KW Jr (2010) Raman scattering in a new carbon material. *Diam Relat Mater* 19(1):31–39
- Wang X, You H, Liu F, Li M, Wan L, Li S, Cheng J (2009) Large-scale synthesis of few-layered graphene using CVD. *Chem Vapor Depos* 15(1–3):53–56
- Wu C, Dong G, Guan L (2010) Production of graphene sheets by a simple helium arc-discharge. *Phys E* 42(5):1267–1271
- Xing G, Jia SL, Shi ZQ (2007) The production of carbon nanomaterials by arc discharge under water or liquid nitrogen. *New Carbon Mater* 22(4):337–341
- Yoshitake T, Shimakawa Y, Kuroshima S, Kimura H, Ichihashi T, Kubo Y, Iijima S (2002) Preparation of fine platinum catalyst supported on single-wall carbon nanohorns for fuel cell application. *Phys B* 323(1–4):124–126